Journal of Molecular Structure 1175 (2019) 39–48

Contents lists available at ScienceDirect

Journal of Molecular Structure

journal homepage: http://www.elsevier.com/locate/molstruc

Synthesis, characterization and biological activities of Ni(II), Cu(II) and UO_2(VI) complexes of N'-((2Z,3E)-3-(hydroxyimino)butan-2-ylidene)-2-phenylacetohydrazide

Şeyma Karadeniz [a], Cigdem Yuksektepe Ataol [b, *], Tevfik Özen [a], Rahim Demir [a], Hatice Öğütçü [c], Hümeyra Bati [a]

[a] Department of Chemistry, Faculty of Art and Sciences, Ondokuz Mayis University, 55139, Samsun, Turkey
[b] Department of Physics, Faculty of Science, Cankiri Karatekin University, 18100, Uluyazi, Cankiri, Turkey
[c] Department of Biology, Faculty of Arts and Science, Ahi Evran University, 40100, Kirsehir, Turkey

ARTICLE INFO

Article history:
Received 14 May 2018
Received in revised form
10 July 2018
Accepted 18 July 2018
Available online 26 July 2018

Keywords:
Hydrazoneoxime
Spectral methods
Antimicrobial
Antioxidant
X-ray

ABSTRACT

In this study, the mononuclear Ni(II), Cu(II) and UO_2(VI) complexes of N'-((2Z,3E)-3-(hydroxyimino) butan-2-ylidene)-2-phenylacetohydrazide ligand (LH_2) have been synthesized. All compounds have been characterized by using elemental, spectral, X-ray analyses and magnetic moment measurements. The IR spectra of Ni(II) and UO_2(VI) complexes show that LH_2 has coordinated to the metal ions in tridentate manner with ON_2 donor sites of deprotonated phenolic −OH, the imine N atoms of hydrazone (CO═N) and oxime (C═N−OH) groups. In the Cu(II) complex, the ligand is ketoamine form and bond to metal ion via carbonyl oxygen, imine nitrogen atoms of oxime and hydrazone groups. The spectral and magnetic studies show that the Ni(II), and Cu(II) complexes exhibit octahedral geometry. UO_2(VI) complex has a monomeric structure constructed of a hexagonal bipyramidal uranyl centre with two monodentate ligand in trans-position. Newly complexes have been tested for antimicrobial and antioxidant activity. All of the complexes have active against *L. monocytogenes*, *M. luteus*, *S. epidermis*, *B. cereus*, *S. typhi H*, *E. coli*, *Klebsiella pneumonia*, *Br. abortus* and *C. albicans*. Results of antioxidant activities indicate that the ligand and complexes have multiple antioxidant activities, such as total antioxidant (phosphomolybdenum) assay, reducing power, free radical (DPPH$^{\bullet}$), superoxide anion and ABTS$^{\bullet+}$ scavenging activity tests. The Ni(II) complex exhibited more effective total antioxidant activity and reducing power than BHA and trolox but weak the ABTS$^{\bullet+}$, free radical (DPPH$^{\bullet}$), and superoxide anion ($O_2^{\bullet-}$) scavenging activity. The ABTS$^{\bullet+}$ and DPPH$^{\bullet}$ scavenging activities of Cu(II) were found excellent in comparison with standards. Ni(II), and UO_2(VI) acted a powerful inhibitor of superoxide anion. The Cu(II) complex crystallized in the monoclinic space group $C2/c$, while UO_2(VI) complex crystallized in the monoclinic space group $P2_1/c$.

1. Introduction

Oxime and hydrazone derivatives are categories of Schiff base compounds that have diverse applications in the analytical, pharmacological and chemical field. In fact, they have shown various biological activities such as analgesic, antimicrobial, antitubercular, anticonvulsant, anti-inflammatory, anti-urease, antitumor, anticancer, antioxidant and corrosion inhibition [1–6]. Metal complexes of Schiff base ligand have revealed preferable enhancement in their activities after complexation as compared to an uncoordinated ligand. The biological relevance of metal complexes has been found to be generally dependent on the nature of the metal ions, its oxidation state, nature and the type of the coordinated ligand and isomers [3]. Developments in the fields of inorganic and bioinorganic chemistry have increased the interest in Schiff base complexes since it has been recognized that many of these complexes may serve as models for mimicking biomolecules [7].

The aroylhydrazones possess a −CONHN═C−R(R_1) (R, R_1 = H or organic group) azomethine group constitute an important class of biologically active molecules that have attracted the interest of medicinal chemists owing to their various biological and pharmaceutical activities such as antifungal, antibacterial, anticancer,

* Corresponding author.
E-mail addresses: yuksektepe.c@karatekin.edu.tr, yuksekc85@gmail.com (C.Y. Ataol).

https://doi.org/10.1016/j.molstruc.2018.07.060
0022-2860/

antioxidant, anti-inflammatory, anti-HIV and anti-tubercular activities [8–11]. The biological activity has been attributed to the complex forming abilities of the ligand with metal ions present in the cells [9]. In some cases, the aroylhydrazonones analogs display micromolar anti-proliferative activity, which is better than that of *cis* platin and bleomycin [10]. Some aroylhydrazones have been widely investigated as one of the orally effective tridentates iron chelators [12]. The coordination compounds of aroylhydrazones are used as models for elucidation the mechanism of enzyme inhibition [12–14].

The oximes and their metal complexes have attracted much attention as they have shown notable bioactivity as chelating therapeutics, as drugs, as inhibitors of enzymes and as intermediates in the biosynthesis of nitrogen oxides [14]. The presence of mild acidic hydroxyl groups and basic nitrogen atoms makes oximes amphoteric ligands [15]. Over the years, oximes have been widely used as very efficient complexing agents in analytical chemistry for isolation, separation and extraction of different metal ions [16]. Numerous aliphatic and aromatic oxime ligands have been shown to possess fungicidal, bactericides, analgesic, antioxidant, antitumor, insecticidal, antiviral, antimalarial, antilepral properties [17,18]. Homo- and heteronuclear Cu(II) and Ni(II) complexes derived from oxime-type ligands have been reported; the observed IC_{50} values indicated that they are potential antioxidant [18]. Among all imine-based reactions, oximes are most stable imines and as a result have found widespread use in applications such as protein labeling, analyzing protein-protein interactions and *in vitro* cell imaging [19].

There is a growing interest in hydrazoneoxime and their coordination compounds because of their biological activity and coordination behavior [18,20]. It was reported that the combination of both oxime and hydrazone groups in the same molecule leads to the formation of more stable chelators by coordination to metal ions [2]. The hydrazone moiety may chelate with metals in ketonamide or deprotonated enolimine form [1]. Such compounds act as tridentate, neutral, mono or biprotic ligands coordinating through the amide oxygen, imine and oxime nitrogens depending on the reaction conditions [20,21]. In hydrazoneoximes, the oxime OH is a very good hydrogen bond donor, while both the oxime oxygen and oxime nitrogen act as hydrogen bond acceptors. In all cases, the oxime nitrogen is a much better hydrogen bond acceptor than the oxime oxygen [20]. Hydrazoneoxime ligands could react with Ni(II) and Cu(II) ions to give mono-and/or binuclear complexes [18].

Diacetyl monoxime and its various derivatives are extensively used as the biologically active, complexing agent and analytical reagent [22]. There are numerous papers on the hydrazones of diacetyl monoxime and their complexes [22–34].

In this paper, we report the synthesis, characterization, spectroscopic properties of Ni(II) (**1**), Cu(II) (**2**) and UO_2(VI) (**3**) complexes of N'-((2Z,3E)-3-(hydroxyimino)butan-2-ylidene)-2-phenylacetohydrazide ligand (LH_2) obtained diacetylmonoxime and phenylaceticacide hydrazide. The antimicrobial activity and antioxidant properties of these compounds were studied. The crystal structures of Cu(II) and UO_2(VI) complexes are also reported by using X-ray technique.

2. Experimental

2.1. Physical measurements

Melting points were determined on an Electrothermal 9100 melting point apparatus. Elemental analyses (C, H, and N) of compounds were obtained from a Thermo FLASH2000 CHNS/O elemental analyzer. UV–vis spectra of 1×10^{-5} M DMSO solutions were recorded on a Thermo Evolution Array Uv–vis spectrophotometer using in the 200–800 nm range. IR spectra were recorded a Perkin Elmer Spectrum Two FT-IR spectrophotometer in the range 4000–400 cm^{-1}. Magnetic measurements were carried out by the MXI Sherwood magnetic susceptibility balance at room temperature.

2.2. X-ray crystallography

X-ray diffraction data of **2,** and **3** were obtained with Stoe IPDS II diffractometer equipped with graphite-monochromated Mo-Kα radiation (λ = 0.71073 Å). The structures were solved by direct methods using SHELXS [35] implemented in the WinGX software system [36] and refined by the full-matrix least-squares procedure on F^2 using SHELXL [37]. All non-hydrogen atoms were easily found from the difference Fourier map and refined anisotropically. All hydrogen atoms in the complexes were included using a riding model and refined isotropically with CH = 0.93 Å, CH_3 = 0.96 Å, CH_2 = 0.97 Å, NH = 0.86 Å, OH = 0.82 Å and OH of the water = 0.85 Å $U_{iso}(H) = 1.5U_{eq}$ (1.2 for methylene group, NH and aromatic ring). Crystallographic data of **2**, and **3**, details of the data collection and structure refinements are listed in Table 1.

2.3. Preparations

2.3.1. Materials

All chemicals purchased from commercial suppliers were of reagent grade and were used without further purification.

2.3.2. Synthesis of ligand LH_2

Ligand, LH_2 was prepared according to the procedure previously described [33].

2.3.3. Synthesis of $[Ni(LH)_2]$ **(1)**

A solution of $Ni(CH_3COO)_2.4H_2O$ (0.249 g, 1.0 mmol) in ethanol (20 mL) was added slowly to a hot solution containing LH_2 (0.466 g, 2 mmol) in ethanol (20 mL). The resulting mixture was refluxed with constant stirring for 5–6 h and then cooled to room temperature. The isolated complex was then filtered off, washed with ethanol and dried in air. Yield: % 45.83, Mp: 262 °C. Elemental Anal. Found (Calcd.) (%): C: 54.87 (55.17), H: 5.41 (5.36), N: 15.89 (16.09).

2.3.4. Synthesis of $[Cu(LH_2)_2]{\cdot}2NO_3{\cdot}2H_2O$ **(2)**

$Cu(NO_3)_2.3H_2O$ (0.242 g, 1 mmol) was added to a 20 mL methanol solution of LH_2 (0.466 g, 2 mmol), and the reaction mixture was stirred for 7 h at room temperature. The resultant dark green solution was filtered and the filtrate was kept in the open air. After 4–5 days, green single crystals suitable for X-ray diffraction analysis were isolated. Yield: % 75.15, Mp:128 °C. Elemental Anal. Found (Calcd.) (%): C: 40.95 (41.77), H: 4.53 (4.97), N: 15.86 (16.24).

2.3.5. Synthesis of $[UO_2(LH)_2]$ **(3)**

A solution of $UO_2(CH_3COO)_2.2H_2O$ (0.424 g, 1.0 mmol) in ethanol (20 mL) was added to a hot solution containing LH_2 (0.466 g, 2 mmol) in ethanol (20 mL). The reaction mixture was refluxed with constant stirring for 5–6 h and the orange solid compounds formed was filtered off, washed with cold ethanol, and dried in air. The bright and orange crystals suitable for X-ray crystallography were obtained from recrystallization of the solid compound in THF solution over a period of 3–4 days. Yield: % 55.35, Mp: 528 °C. Elemental Anal. Found (Calcd.) (%): C: 38.45 (39.23), H: 3.56 (3.81), N: 10.85 (11.44). Chemical structures of **1**, **2**, and **3** are shown from Scheme 1.

Table 1
Crystallograhic data for **2**, and **3**.

Molecules	2	3
Empirical formula	$C_{24}H_{30}CuN_6O_4.2(NO_3).2(H_2O)$	$C_{24}H_{28}UN_6O_6$
Molecular weight	690.13	734.55
Temperature, T (K)	150	296
Wavelength (Å)	0.71073	0.71073
Crystal system	Monoclinic	Monoclinic
Crystal size (mm^3)	0.160 × 0.307 x 0.440	0.09 × 0.11 x 0.15
Space group	C 2/c	$P2_1/c$
a (Å)	21.7159(11)	12.6921(14)
b (Å)	14.5797(6)	8.8796(5)
c (Å)	9.2109(4)	16.3763(17)
α (°)	90.00	90
β (°)	94.384(4)	133.964(6)
γ (°)	90.00	90
Volume, V ($Å^3$)	2907.7(2)	1328.4(2)
Z	4	2
Calculated density (Mg m^{-3})	1.576	1.836
θ Range (°)	2.22–28.07	2.2–26.00
Index ranges	h = −21 → 25, k = −17 → 16, l = −10 → 10	h = −15 → 15, k = −10 → 10, l = −20 → 20
Measured reflections	5675	9213
Independent reflections	2539	2606
Observed reflections, (I > 2σ)	2201	1833
Goodness-of-fit on F^2	1.026	1.044
R_1 indices (I > 2σ)	0.03	0.03
wR_2 indices (I > 2σ)	0.08	0.06
CCDC Number	1580665	1578847

2.4. Antimicrobial activity

Antimicrobial activities of complexes were tested by well-diffusion metod [38]. The bacterial subcultures chosen were *Listeria monocytogenes* 4b ATCC19115, *Staphylococcus aureus* ATCC25923, *Escherichia coli* ATCC1280, *Salmonella typhi* H NCTC901.8394, *Brucella abortus* RSKK03026, *Staphylococcus epidermis* sp., *Micrococcus luteus* ATCC9341, *Pseudomonasa eroginosa* sp. ATCC19115, *Klebsiella pneumonia* ATCC 27853, *Proteus vulgaris* RSKK 96026, *Serratia marcescens* ATCC81003 and *Bacillus cereus* RSKK863. An antifungal susceptibility test was performed using *Candida albicans* Y-1200-NIH, Tokyo.

2.5. In vitro antioxidant assays

The EC_{50} and IC_{50} values were calculated by plotting the linear regression graphs where the abscissa represents the different concentrations of the test sample while the ordinate represents the measured results (absorbance) from three separate tests. BHA and Trolox were used as reference standards.

2.5.1. Total antioxidant (phosphomolybdenum) assay

The total antioxidant activity of compound was determined by the phosphomolybdenum method as previously described [39]. The method was evaluated by the activity to convert Mo^{6+} into Mo^{5+}, measuring the absorbance at 695 nm, spectrophotometrically. The antioxidant activity was expressed the EC_{50} value as $A_{0.50}$, that corresponds to the concentration providing 0.500 absorbance.

2.5.2. Reducing power

The reducing power was performed by adopted method with slight modifications [40]. This method was evaluated by the activity to convert Fe^{3+} into Fe^{2+}, measuring the absorbance at 700 nm, spectrophotometrically. The reducing power was given as $A_{0.50}$ that corresponds to the concentration providing 0.500 absorbance.

2.5.3. Free radical scavenging activity

The electron donation capacity of the compounds was evaluated by bleaching of free radical (DPPH$^{\bullet}$ 1,1-diphenyl-2-picrylhydrazyl radical) described method [41] wherein the bleaching level of a stable DPPH$^{\bullet}$. The reduction of the DPPH$^{\bullet}$ testing free radical scavenging activity was monitored at 517 nm.

2.5.4. Superoxide anion scavenging activity

The superoxide anion scavenging activity of compounds was determined using system as described earlier [42]. The scavenging of the superoxide anion was measured at 532 nm.

2.5.5. $ABTS^{\bullet+}$ scavenging activity

$ABTS^{\bullet+}$ radical cation scavenging activity is based on the antioxidant activity of compounds to scavenge $ABTS^{\bullet+}$ and reduce $ABTS^{\bullet+}$ by antioxidants. The activity of compounds to scavenge $ABTS^{\bullet+}$ was evaluated by modified method [43].

2.5.6. Statistical analysis

All antioxidant tests were performed in triplicate and obtained averages of all results (mean ± SD). The EC_{50} and IC_{50} values were calculated by linear interpolation between the values registered above and below 50% activity. Data were analysed by an analysis of variance, $p < 0.05$.

3. Results and discussion

3.1. Structure description of the complexes *2* and *3*

The molecular structures of the complex $[Cu(LH_2)_2]\cdot 2NO_3\cdot 2H_2O$ (**2**) and $[UO_2(LH)_2]$ (**3**) were determined to confirm the assigned structures and establish conformation of the molecules. ORTEP drawings of **2** and **3** with atomic numbering are shown in Fig. 1a and Fig. 1b.

The structures **2** and **3** crystallize in monoclinic space groups C 2/c and $P2_1/c$, respectively. The compound **2** containing arolyhydrazone and oxime groups crystallizes in ketoamine form while the compound **3** crystallizes in enolimine form (Scheme 1 and Fig. 1). The compounds **2**, and **3** are coordinated enolate oxygen, oxime nitrogen, and amine/imine nitrogen atoms of two the tridentate

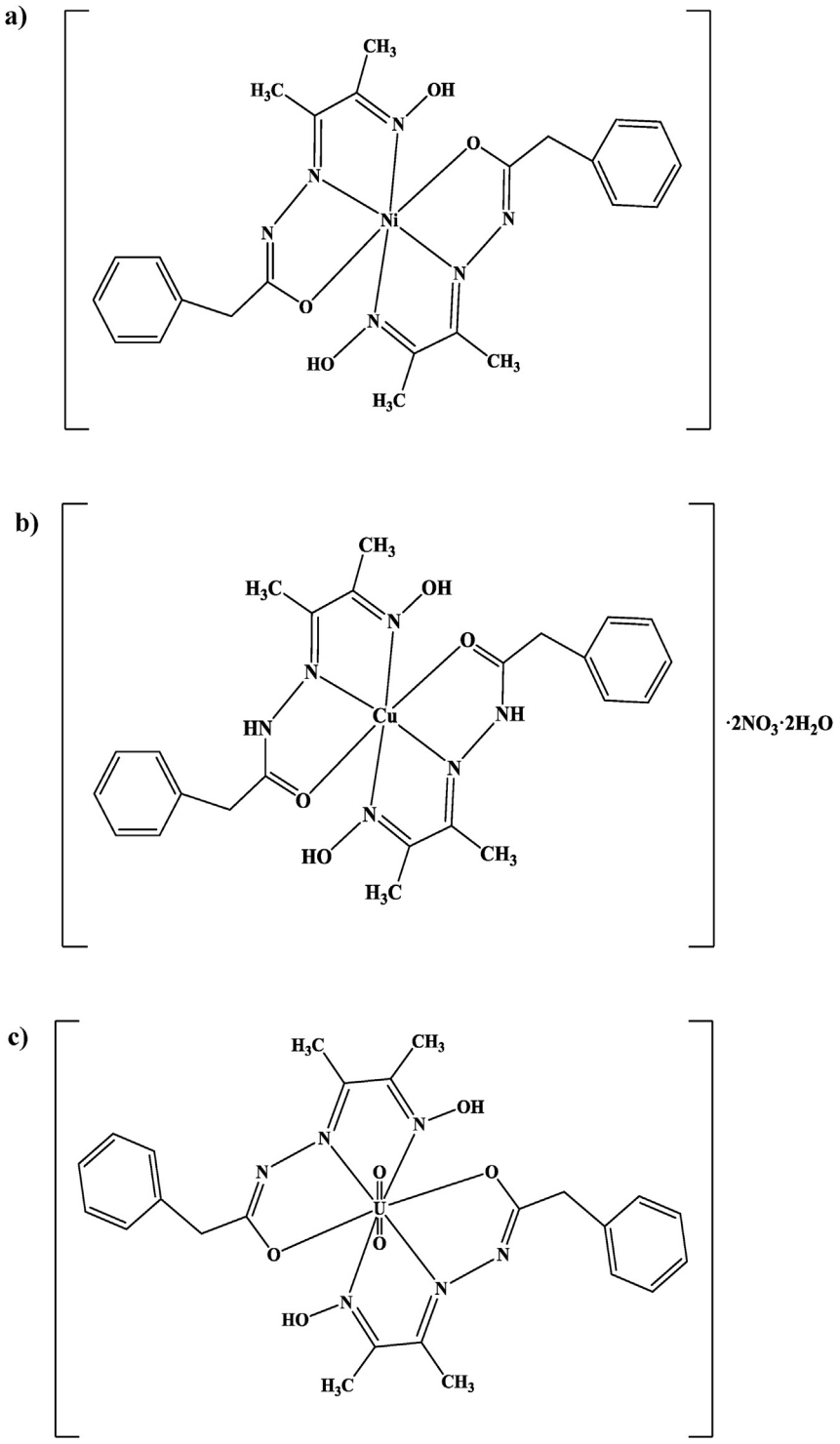

Scheme 1. Chemical structures of the complexes **a)** for **1, b)** for **2,** and **c)** for **3**.

keto/enol forms, respectively and also, there are two water molecules and nitrate group in the structure **2**. The Cu(II) metal ion bonds with O(2), N(2), N(3), and $N(2)^{i}$ atoms in the basal plane and $O(2)^{i}$ and $N(3)^{i}$ atoms fillings the axial positions while UO_2(VI) metal ion bonds with O(2), N(2), N(3), $O(2)^{iv}$, $N(2)^{iv}$, $N(3)^{iv}$, atoms in the basal plane and O(3) and $O(3)^{iv}$ atoms fillings the axial positions. The local coordinations of copper(II) and uranium(VI) are an almost perfect octahedral and hexagonal bipyramid environment, the sum of angles being 359.97° (O(2)–Cu–N(2), O(2)–Cu–$N(2)^{i}$, N(3)–Cu–N(2) and N(3)–Cu–$N(2)^{i}$) and 360.00° ($O(2)^{iv}$–U–O(3), O(2)–U–O(3), O(2)–U–$O(3)^{iv}$ and $O(2)^{iv}$–U–$O(3)^{iv}$), respectively. The ligand: metal ratios were 2:1 for mononuclear **2** and **3** complexes, respectively.

As can be seen from Table 2, The C(5)–O(2) bond is a double bond in compound **2**, while in bond **3** it is converted to a single bond since bond length is increased. Likewise, the C(5)–N(1) bond

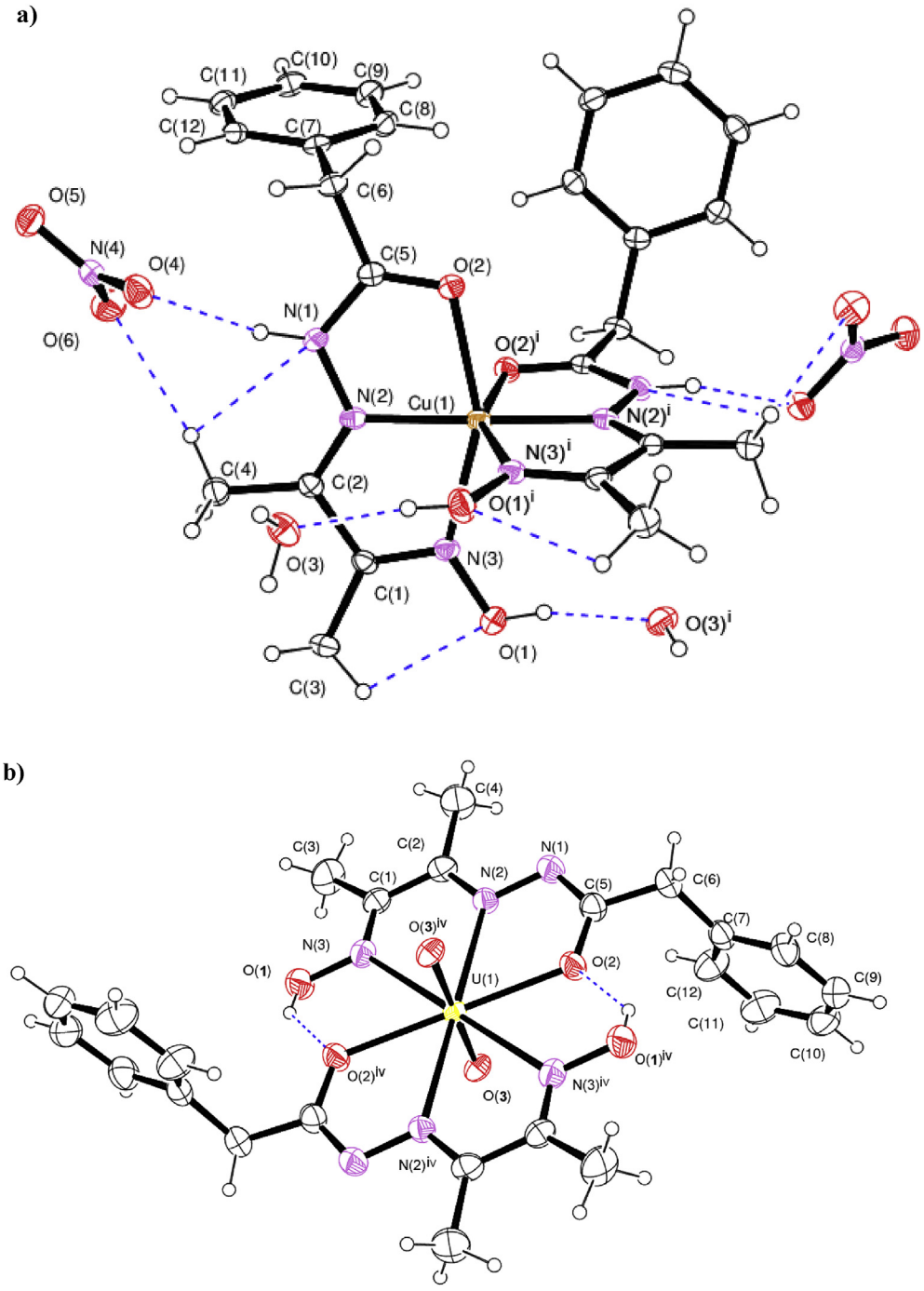

Fig. 1. Ortep drawing of the structures **a)** for **2,** and **b)** for **3**.

is a single bond in compound **2**, while it is converted to a double bond in the complex **3**. In the compound **2**, it is found that the bond lengths of Cu–$N(2)_{amine}$, Cu–$N(3)_{oxime}$, and Cu–$O(2)_{enolate}$ are being 1.947(2), 2.168(2), and 2.155(2), respectively. As can be seen from Table 3, X-ray results show the intra molecular hydrogen bonds between the methyl and nitrate groups in the complex structure **2** and the Schiff base, nitrate, oxime, and water. In the compound **3**, it is found that the bond lengths of U–$N(2)_{imine}$, U–$N(3)_{oxime}$, U–$O(2)_{enolate}$ and U–O(2) are being 2.621(4), 2.665(5), 2.370(4) and 1.751(4) Å, respectively. the C(5)–N(1)–N(2)–C(2) torsional angles are being −178.52(19), and −179.5(5) for **2**, and **3**, respectively. The complexes **2**, and **3** were found to be compatible with similar studies in the literature [33].

It can be seen from Table 3 that the compound **2** have five intramolecular C–H···O/N, N–H···O and O–H···O with intermolecular O–H···O hydrogen bonds but the compound **3** has an intramolecular O–H···O hydrogen bond. As can be seen from Fig. 1a and b, in the compound **2** the intramolecular hydrogen bonds are between the solvent water molecules and oxime O atom with nitrate group and methyl with hydrazone amine groups while in the

Table 2
The related bond distances (Å) and angles (°) of **2** and **3** (Symmetry codes: (i): x, y, ½-z; (iv): 1-x, -y, -z).

2		**3**	
N(3)–O(1)	1.371(2)	N(3)–O(1)	1.385(6)
C(1)–N(3)	1.291(3)	C(1)–N(3)	1.284(7)
C(1)–C(2)	1.494(3)	C(1)–C(2)	1.443(8)
C(2)–N(2)	1.280(3)	C(2)–N(2)	1.285(7)
N(1)–N(2)	1.378(3)	N(1)–N(2)	1.387(6)
C(5)–N(1)	1.354(3)	C(5)–N(1)	1.318(7)
C(5)–O(2)	1.235(3)	C(5)–O(2)	1.293(7)
Cu–N(2)	1.947(2)	U–N(2)	2.621(4)
Cu–N(3)	2.168(2)	U–N(3)	2.665(5)
Cu–O(2)	2.155(2)	U–O(2)	2.370(4)
C(1)–N(3)–O(1)	113.20(18)	U–O(3)	1.751(4)
C(2)–C(1)–N(3)	114.67(19)	C(1)–N(3)–O(1)	113.8(5)
N(2)–C(2)–C(1)	114.3(2)	C(2)–C(1)–N(3)	115.2(5)
N(1)–N(2)–C(2)	123.96(19)	N(2)–C(2)–C(1)	116.7(5)
C(5)–N(1)–N(2)	115.95(18)	N(1)–N(2)–C(2)	115.0(5)
O(2)–C(5)–N(1)	120.45(19)	C(5)–N(1)–N(2)	109.7(4)
O(2)–Cu–N(3)	154.88(7)	O(2)–C(5)–N(1)	123.0(5)
O(2)–Cu–N(2)	78.11(7)	O(2)–U–N(3)	117.90(14)
N(2)–Cu–N(3)	76.77(7)	O(2)–U–N(2)	92.28(16)
N(2)–Cu–N(3)^{i}	104.23(7)	N(2)–U–N(3)	58.34(14)
N(2)–Cu–O(2)^{i}	100.86(7)	N(2)–U–O(3)	59.84(13)
O(2)–Cu–N(3)^{i}	98.27(6)	O(2)–U–O(3)	89.31(16)
O(2)–Cu–O(2)^{i}	85.77(8)	N(3)–U–O(3)	87.71(15)
N(3)–Cu–N(3)^{i}	88.56(10)	N(2)–U–N(3)^{iv}	121.66(14)
N(2)–Cu–N(2)^{i}	178.63(10)	N(2)–U–O(2)^{iv}	120.16(13)
		N(2)–U–O(3)^{iv}	87.72(16)
		O(2)–U–N(3)^{iv}	62.10(14)
		O(2)–U–O(2)^{iv}	180.0
		N(3)–U–N(3)^{iv}	180.0
		N(2)–U–N(2)^{iv}	180.00(19)
		O(2)–U–O(3)^{iv}	90.69(16)
		N(3)–U–O(3)^{iv}	92.29(15)

Table 3
Hydrogen bond interactions of the title compounds **2,** and **3** (Å, °).

Hydrogen bond(Å,°)	D–H	H … A	D … A	D–H … A
2				
C(4)–H(4A) … O(6)	0.96	2.51	3.419(3)	157
C(4)–H(4A) … N(1)	0.96	2.53	2.922(3)	104
C(3)–H(3A) … O(1)	0.96	2.32	2.678(3)	101
N(1)–H(1A) … O(4)	0.86	2.07	2.871(3)	155
O(1)–H(1) … O(3)^{i}	0.82	1.86	2.665(3)	166
O(3)–H(3WA) … O(5)^{ii}	0.85	2.03	2.875(3)	174
O(3)–H(3WB)···O(4)^{iii}	0.85	2.33	3.147(3)	160
O(3)–H(3WB)···O(5)^{iii}	0.85	2.32	3.04682)	144
3				
O(1)–H(1) … O(2)^{iv}	0.82	1.83	2.488(6)	136

Symmetry codes: (i): x, y, 1/2-z; (ii): 1/2-x, 1/2 + y, 1/2-z; (iii): 1/2-x, 1/2-y, 1-z; (iv): 1-x, -y, -z.

compound **3** the intramolecular hydrogen bonds are between the oxime atoms and enolate O atoms.

As can be seen from Fig. 2a, the molecules with two different symmetry codes ((x, y, z) and (1/2-x,1/2 + y,1/2-z)) are linked to each other by the solvent water group and the nitrate group. The solvent water and nitrate groups serve as a bridge between the two molecules. In Fig. 2a, the chain O(1)^{i}–H(1)^{i} … O(3)–H(3WA) … O(5)^{ii}–N(4)^{ii}–O(4)^{ii} … H(1A)^{ii}–N(1)^{ii} is seen as intermolecular hydrogen bonds. In this chain, the oxime, water and nitrate groups bond with the water molecule, nitrate group and hydrazone amine group, respectively. In Fig. 2b, it is seen that the intermolecular O–H···O hydrogen bonds between the water and nitrate groups are centered at (1/4, 1/4, 1/4) and characterized by an $R_6^6(24)$ motif ($R_d^a(r)$: R is a ring in the intermolecular hydrogen bond, d is the number of the donor atoms in the ring, a is the number of the acceptor atoms in the ring and r is the number of the total atoms in the ring) [44,45]. The $R_6^6(24)$ rings formed by hydrogen bond are centered at [n+1/4, k+1/4, l+1/4] (n, k, and l are zero or integer).

3.2. *Infrared spectra of **(1), (2)** and **(3)***

The ligand bonding modes in complexes have been deduced by comparing the complexes IR spectra with parent ligand spectra. The characteristic absorption bands due to ν(N − H) and ν(C = O), which appeared around 3198 cm^{-1} and 1671 cm^{-1} respectively, in the IR spectra of free ligand, disappeared completely in spectra of complexes **1** and **3,** and two new bands due to conjugate system ν(−C = N − N = C −) and ν(C − O) appeared in the regions 1527, 1587 and 1182, 1176 cm^{-1}, respectively [1,46]. This is a clear evidence of enolization of ligand during complexation [29]. The free ligand shows bands at 3308, 1020 and 975 cm^{-1} due to ν(O − H) $_{(oxime)}$, ν(N − O) and ν(N − N), respectively. These values are in accord with the previously reported hydrazoneoxime derivatives [1,14,23]. Both elemental analyses and IR spectral data of **1** and **3** indicate that the ligand (LH_2) [33] behaves as a mononegative tridentate ligand linked with metal ion via oximino nitrogen, hydrazone imine nitrogen atom and deprotonated enolimine oxygen while oxime residue remains protonated [47]. The new bands at 923 and 789 cm^{-1} are observed in spectra of complex 3 which are assigned to $\nu(UO_2)_{as}$ and ν_s (O═U═O) modes, respectively [48].

In the IR spectra of **2**, a broad absorption band around 3387 cm^{-1} attributed to O–H stretching vibration of crystal water. The spectrum shows also vibrational bands at 1622, 1598 and 1585 cm^{-1} assigned for ν (C = O), ν $(C = N)_{imine}$ and ν $(C = N)_{oxime}$, respectively (see Fig. 3). These values show that ligand is in neutral keto-amine form, which bonded to metal ion via carbonyl oxygen, imine nitrogen atoms of oxime and hydrazone groups. The tautomeric form of ligand in their metal complexes is highly dependent on the pH of the medium and the neutral of metal ions. It reported that, Cu(II) complexes of Schiff base are in keto form, by using of

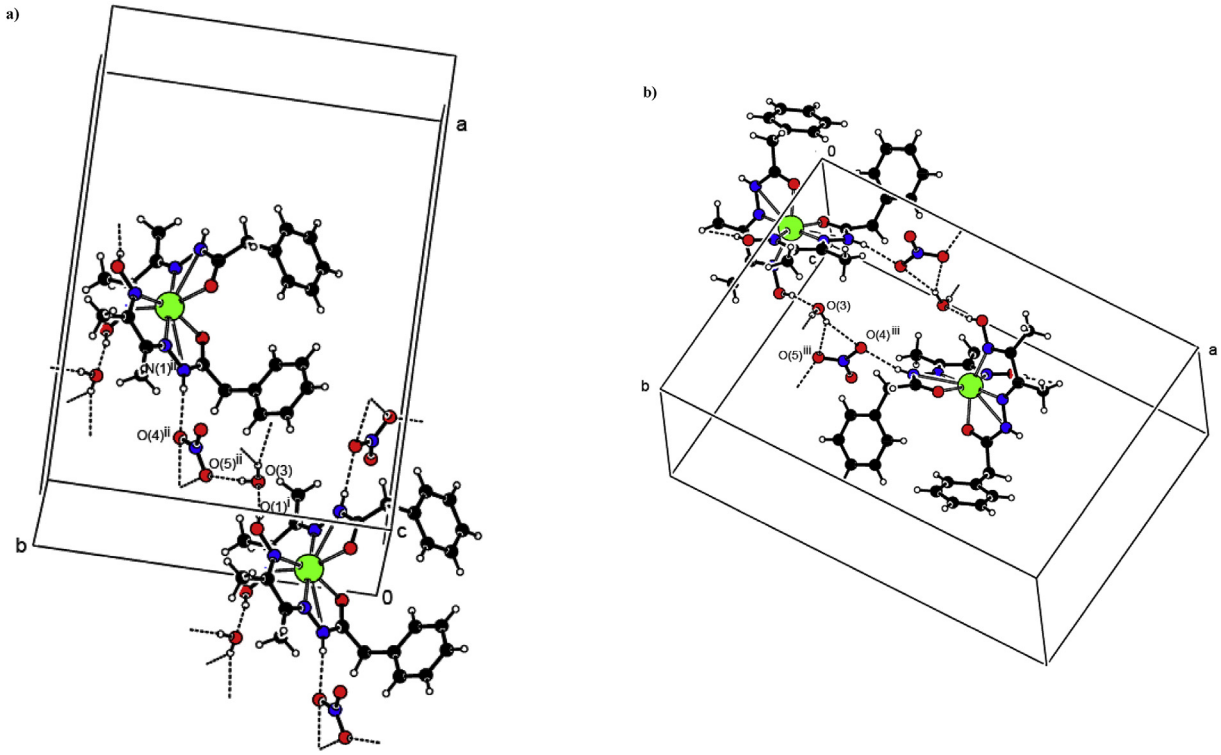

Fig. 2. Crystal packing of the structures for **2 a)** O(3)–H(3WA) … O(5)^{ii}, **b)** O(3)–H(3WB)···O(4)^{iii}, and O(3)–H(3WB)···O(5)^{iii} (Symmetry codes: (ii): 1/2-x, 1/2 + y, 1/2-z; (iii): 1/2-x, 1/2-y, 1-z).

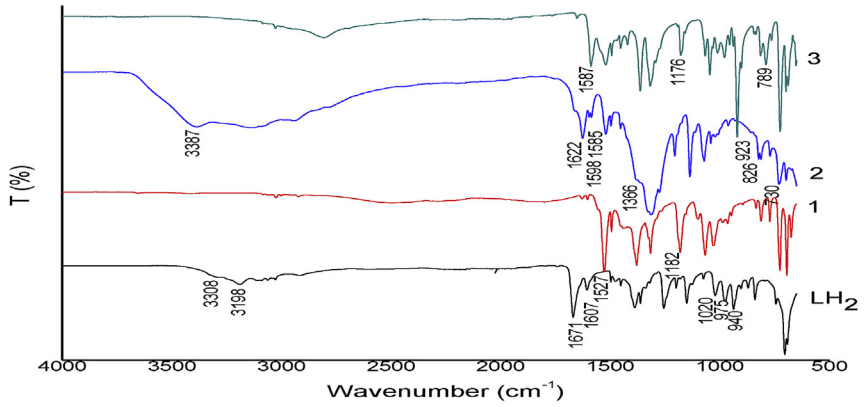

Fig. 3. Infrared spectra of **LH_2** [33], complexes **1**, **2** and **3**.

salts derived from strong acids, such as $Cu(NO_3)_2.2.5H_2O$, $CuCl_2.2H_2O$ and $CuSO_4.5H_2O$, without the presence of any additional base [49]. Bands near 1366, 826 and 730 cm^{-1} in **2** indicate that the nitrate group is ionically bonded [50].

3.3. *Uv spectra and magnetic studies of **(1)**, **(2)** and **(3)***

The electronic spectrum of ligand shows three bands at 270, 290 and 319 nm, the first two bands may be assigned to $\pi \rightarrow \pi^*$ transitions of aromatic ring which is nearly unchanged upon complexation, whereas the third band may be assigned to the $n \rightarrow \pi^*$ electronic transition of imine and carbonyl groups [33] (Fig. 4). The **1** shows one band in spectra at 450 nm, which may be assigned $^3A_{2g} \rightarrow {}^3T_{2g}(P)$, suggesting an octahedral geometry for the Ni(II) complex [14]. The other two d-d transition in this type of complexes may appear above 500 nm but does not appear due to the low intensity of d-d transition [51]. A broad and very strong bands observed in the region of 350 nm are attributed to ligand → metal charge transfer transition. The magnetic moment recorded for **1** was 2.95 B M. which was in the expected range of octahedral geometry around the central metal ion [14] (Table 2). The **2** shows an absorption around 678 nm assigned to $^3E_g \rightarrow {}^3T_{2g}$ transition, suggesting an octahedral geometry for Cu(II) complex [17]. The **2** is paramagnetic and magnetic moment was 1.68 B. M., corresponding to one unpaired electron in an octahedral geometry [14]. The electronic spectra of **3** shows two bands, in addition to ligand bands. The first band is observed at 360 nm corresponding to charge transfer from equatorial donor atoms of ligand to uranyl ion. The second band is observed at 450 nm due to electronic transition from oxygen atom of uranyl moiety to the f-orbital of uranium (VI)

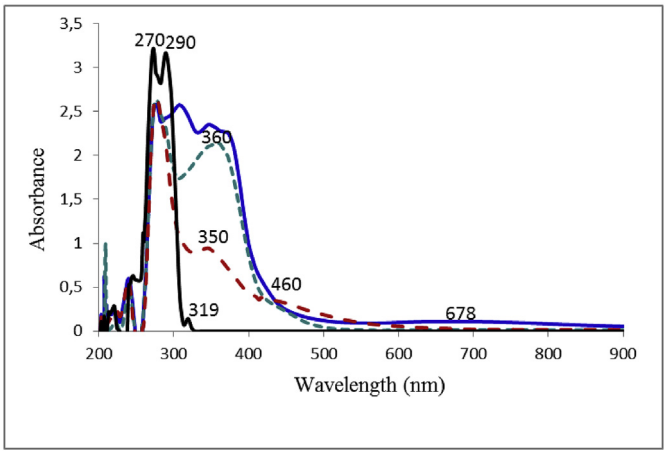

Fig. 4. Uv–vis spectra of **LH_2** [33], complexes **1**, **2** and **3**.

ion (O → U) [2,52]. The **3** was found to be diamagnetic as expected and did not give any significant values for the magnetic moment.

3.4. Antimicrobial activity

The dramatically rising prevalence of multi-drug resistant microbial infections in past few decades has become a serious health care problem. The search for new antimicrobial agents will consequently always remain as an important and challenging task for medicinal chemistry. The antimicrobial activities of ligand and its metal complexes were screened at different concentrations (100 and 200 μg/mL) in DMSO solvent as a control substance by using disc diffusion method agains Gram (+) (*L. monocytogenes, M. luteus, S. aureus, S. epidermis, B. cereus),* Gram (−) (*E. coli, Br. abortus, P. Aeroginosa, S. typhi H, Klebsiella pneumonia, Proteus vulgaris, Serratia marcescens*) and one yeast. All the synthesized compounds and antibiotic exhibited the varying degree of inhibitory effects on the growth of different tested strains (Table 4). All the compounds were active against *L. monocytogenes*, *M. luteus*, *S. epidermis*, *B. cereus, S. typhi H*, *E. coli*, *K. pneumonia*, *Br. abortus* and *C. albicans*. *Br. abortus* is a gram-negative bacterium that causes premature abortion of a cattle fetus. What makes this bacterium so dangerous is that it can be transferred from an animal to a human host [38]. In humans, *B. abortus* induces severe illnesses involving fever, malaise, anorexia, depression, physical weakness, weight loss, headache and bone and muscle pain, but can be treated with antibiotics. This study indicates that **1**, **2** and **3** complexes of hydrazone oxime ligand at high concentration are more active against *Br. abortus* and *M. luteus*. Only high concentrations of **1** and **2** are effective against *S. marcescens*, which is an important cause of nosocomial infections in both human and veterinary medicine (Table 4). **1** against *E. coli* and **2** against *S. typhi H* were observed to be as effective as K30 at high concentrations. In general, the metal complexes are more potent bactericides than the ligand. This enhancement in activity may be explained on the basis of chelation theory Chelation reduces the polarity of the metal ion. Hence, a complex has lipophilic character and increases the interaction between metal ion and the lipid is favored. This lead to the breakdown of the permeability barrier of the cell, resulting in interference with the normal cellular processes [38].

Furthermore, the antibacterial activity of these compounds was also compared with seven commercial antibiotics, namely kanamycin, sulfamethoxazole, ampicillin, ciprofloxacin, amoxycillin, sulbactam, and nystatin. It was seen that the synthesized compounds were effective as the antibiotics mentioned.

3.5. Antioxidant activity

In the current investigation, the *in vitro* antioxidant activities of the newly synthesized compounds were evaluated widely used for *in vitro* studies to investigate the antioxidant assays such as total antioxidant (phosphomolybdenum) assay, reducing power, free radical (DPPH$^{\bullet}$), superoxide anion and ABTS$^{\bullet+}$ scavenging activity tests, the lowest EC_{50} and IC_{50} values represent the highest activity.

Phosphomolybdenum assay: For **LH_2**, **1**, **2** and **3**, total antioxidant activity was determinated by phosphomolybdenum method [39,53]. For this assay, solutions of different concentrations for each of the compounds were used to find EC_{50} values (Table 5). The EC_{50} values were in good agreement with standards and indicated that the compounds possessed significant total antioxidant activity. However, total antioxidant activities of LH_2 1, 2, and 3 according to

Table 4
Antimicrobiyal activity of studied compounds (100 and 200 μg/mL) and standard reagents (diameter of zone inhibition, mm).

Microorganisms		LH_2	1	2	3	Control
		200/100 μg/mL				
Gram (+)	L.monocytogenes	–/–	20/25	20/20	24/20	–
	M.luteus	17.5/19.5	19/16	19/18	25/18	–
	S.aureus	22.5/20	15/24	–/–	–/–	–
	S.epidermis	17.5/17.5	15/20	18/16	16/16	–
	B.cereus	20/20.5	15/17	18/19	15/16	–
Gram (−)	*Br.abortus*	–/–	21/-	18/16	20/15	–
	P. aeroginosa	15/19	20/25	–/–	20/22	
	S.typhi H	18.5/16	18/15	24/13	15/17	–
	E.coli	17.5/16.5	25/20	15/20	14/18	–
	K. pneumonia	-/7.5	17/20	25/20	17/16	–
	P. vulgaris	–/–	–/–	-/20	–/–	–
	S. marcescens	–/–	25/-	–/–	25/-	–
Yeast	*C. albicans*	27/25	27/32	30/30	30/25	–
Pozitif Control	***S.aureus***	***P.putida***	***E.coli***	***S.typhi H***	***Br. abortus***	***C.albicans***
K30	25	14	25	20	–	–
SXT25	24	18	18	17	–	–
AMP10	30	8	10	11	–	–
AMC30	30	15	14	19	–	–
NYS100	–	–	–	–	–	20

K30 Kanamycin 30 lg, SXT25 Sulphamethoxazol 25 lg, AMP10 Ampicillin 10 lg, AMC30 Amoxycillin 30 lg, NYS100 Nystatin 100 lg.

Table 5
In vitro antioxidant activities of LH_2, **1**, **2** and **3** compared with BHA and Trolox in phosphomolybdenum, reducing power, DPPH$^{\bullet}$, $O_2^{\bullet-}$ and ABTS$^{\bullet+}$ scavenging methods.

Sample	*In vitro* Antioxidant Assays*				
	A EC_{50}, μg/mL	B EC_{50}, μg/mL	C IC_{50}, μg/mL	D IC_{50}, μg/mL	E IC_{50}, μg/mL
LH_2	40.25 ± 8.44	32.76 ± 9.47	0.0037 ± 0.0009	9.42 ± 0.30	8.15 ± 0.08
1	38.38 ± 1.67	14.17 ± 0.13	0.2919 ± 0.184	0.0214 ± 0.0037	12.85 ± 0.02
2	49.52 ± 1.96	17.13 ± 3.06	0.0082 ± 0.0011	7.51 ± 0.14	11.55 ± 1.35
3	36.73 ± 1.10	19.7 ± 3.13	0.0101 ± 0.0085	0.047 ± 0.0009	18.62 ± 3.51
BHA	30.60 ± 0.17	36.54 ± 3.07	0.0013 ± 0.0009	0.16 ± 0.02	0.17 ± 0.03
Trolox	32.69 ± 2.34	40.89 ± 1.42	0.0027 ± 0.0008	4.98 ± 1.17	0.0046 ± 0.0015

*Values represent mean ± S.D.
**The syntheses of LH_2 used in this work, have been described in literature [33].
A: Phosphomolybdenum assay, effective concentration (EC_{50}) at which the absorbance is $A_{0.5}$.
B: Reducing power, effective concentration (EC_{50}) at which the absorbance is $A_{0.5}$.
C: Free radical (DPPH$^{\bullet}$) scavenging activity, 50% inhibitory concentration (IC_{50}).
D: Superoxide anion ($O_2^{\bullet-}$) scavenging activity, 50% inhibitory concentration (IC_{50}).
E: ABTS$^{\bullet+}$ scavenging activity, 50% inhibitory concentration (IC_{50}).

EC_{50} values were found higher than standards. The trend observed in EC_{50} values were BHA (30.60 μg/mL) < Trolox (32.69 μg/mL) < **3** (36.73 μg/mL) < **1** (38.38 μg/mL) < **LH_2** (40.25 μg/mL) < 2 (49.52 μg/mL).

Reducing power: The reducing capacity of a compound may help to decide as a significant indicator of its potential antioxidant activity [54]. Reducing power capacities expressed as EC_{50} (the concentration at which the absorbance is $A_{0.50}$) of **LH_2**, **1**, **2** and **3** were given in Table 5. Hydrazoneoxime ligand and its complexes were able to reduce Fe^{3+} to Fe^{2+} transformation and also monitored spectrophotometrically at 700 nm [53]. EC_{50} was calculated at the different concentration at which the absorbance is 0.50. The results differed between synthesized compounds and standards, significantly ($p < 0.05$). BHA and Trolox have the highest EC_{50} value as standards, that is, the lowest reducing power capacity. EC_{50} values of the oxime complexes and ligand have effective reducing power capacities than BHA and Trolox. The reducing power (EC_{50}) of **LH_2**, **1**, **2** and **3** BHA and Trolox were in the following order: Trolox > BHA > LH_2 > 3 > 2 > 1.

Free radical scavenging activity: Free radical (DPPH$^{\bullet}$) scavenging activity determination method is cheap, simple and fast and therefore, it is used in the analysis of compounds. In this assay, the pink DPPH$^{\bullet}$ takes place by reducing or antioxidant molecules providing light yellow hydrazine formation and is measured at 517 nm [55]. The DPPH· scavenging activity of the compound and complexes have been investigated and the obtained IC_{50} are presented in Table 5. The reaction between the DPPH· and samples using BHA and Trolox as standard antioxidants under the similar test conditions was measured by decreasing in absorbance (517 nm), spectrophotometrically. The **1** (IC_{50} = 0.2919 μg/mL), **2** (IC_{50} = 0.0082 μg/mL) and **3** (IC_{50} = 0.0101 μg/mL) and ligand (IC_{50} = 0.0037 μg/mL) have showed good free radical scavenging activities of IC_{50} values comparable with that of BHA (IC_{50} = 0.0013 μg/mL) and Trolox (IC_{50} = 0.0027 μg/mL). The lower value of IC_{50} means the high antiradical activity for complexes and ligand. The order of free radical scavenging activity for ligand, complexes and standards increases in the order: **1** > **3** > **2** > **LH_2** > Trolox > BHA.

Superoxide anion scavenging activity: Superoxide radicals may interact with macromolecules such as lipids, proteins, and DNA to produce more effective species together with $^1O_2$, H_2O_2 and $^{\cdot}OH$ [56]. Thus, elimination of oxidative stress source superoxide anions is very important in the prevention of many diseases. Superoxide anion formed by PMS–NADH reduces NBT in this assay. In this test, superoxide anion reduces the yellow pigment (NBT^{+2}) to produce the blue-formazan which is monitored at 560 nm spectrophotometrically [57]. The effective antioxidant inhibits formazan formation. All synthesized complexes and ligand were evaluated for their superoxide anion scavenging activities. As shown in Table 5, all samples exhibited measurable superoxide anion activity. In particular, **1** and **3** exhibited potent superoxide anion activity, with IC_{50} values of 0.0214 μg/mL and 0.047 μg/mL, respectively. The lower values of IC_{50} means high superoxide anion scavenging activity for complexes and ligand. The order of superoxide anion scavenging activity for ligand, complexes and standards increases in the order: **LH_2** > **2** > Trolox > BHA > **3** > **1**.

$ABTS^{\cdot+}$ scavenging activity: The $ABTS^{\cdot+}$ was obtained by an oxidation reaction with potassium persulfate. In the present case, the reduction of $ABTS^{\cdot+}$ occurs in the presence of a hydrogen-capable compound and the product was quantitatively measured at 734 nm by recording the absorbance value [58]. In the $ABTS^{\cdot+}$ assay, **1, 2, 3 and LH_2** exhibited prominent $ABTS^{\cdot+}$ scavenging activity (Table 5). The overall trend observed in level of $ABTS^{\cdot+}$ scavenging for ligand and complexes was found as LH_2 (8.15 μg/mL) > **3** (18.62 μg/mL) > **1** (12.85 μg/mL) > **2** (11.55 μg/mL) > BHA (0.17 μg/mL) > Trolox (0.0046 μg/mL).

4. Conclusion

This work includes the synthesis and characterization of the mononuclear Ni(II), Cu(II) and UO_2(VI) complexes derived N'-((2Z,3E)-3-(hydroxyimino)butan-2-ylidene)-2-phenylacetohydrazide ligand. The compounds (**1**–**3**) have been investigated by spectroscopic methods, magnetic moments, and X-ray diffraction analysis. IR spectra and X-ray diffraction results show that the ligand is coordinated through enolate oxygen, oxime nitrogen and the imine nitrogen atoms as a monobasic O, N, N-tridentate ligand for **1** and **3**. The ligand in the **2** is keto-amine form. The **2** and **3** are an almost perfect octahedral and hegzogonal bipyramid environments, respectively. The newly synthesized compounds were found to have antimicrobial activity against *L. monocytogenes*, *M. luteus*, *S. epidermis*, *B. cereus*, *S. typhi H*, *E. coli*, *K. pneumonia*, *Br. abortus* and *C. albicans*. The antioxidant capacity was performed using *in vitro* assays: phosphomolybdenum assay, reducing power, free radical (DPPH$^{\bullet}$), superoxide anion ($O_2^{\bullet-}$) and $ABTS^{\cdot+}$ scavenging assays. All of the complexes showed improved antioxidant effects in comparison to the corresponding BHA and Trolox. A effective antiradical activity (DPPH$^{\bullet}$, $O_2^{\bullet-}$ and $ABTS^{\cdot+}$) was exhibited by **1** and **2**. The **1** and **2** had also a good phosphomolybdenum (Mo^{6+} to Mo^{5+}) reducing and reducing power (Fe^{3+} to Fe^{2+}). The results of this work support the antioxidant potential of **1** and **2,** and also motivate *in vivo* inhibition and antioxidant research.

Conflicts of interest

The authors declare no conflict of interest, financial or otherwise.

Acknowledgements

The authors acknowledge Scientific and Technological Research Application and Research Centre, Sinop University, Turkey, for the use of the Bruker D8-QUEST diffractometer.

Supplementary Data

Crystallographic data for the structural analysis have been deposited with the Cambridge Crystallographic Data Centre, CCDC No 1580665 for **2** and 1578847 for **3.** Copies of this information may be obtained free of charge from the Director, CCDC, 12 Union Road, Cambridge CB2 1EZ, UK (fax: +44-1223-336033; e-mail: deposit@ccdc.cam.ac.uk or www: http://www.ccdc.cam.ac.uk).

References

[1] M.M. Al Ne'aimi, M.M. Al-Khuder, Spectrochim. Acta Part A-M. 105 (2013) 365.
[2] F.A. El-Saied, A.N. Al-Hakimi, W.A. Wahba, M.M.E. Shakdofa, Egypt. J. Chem. 60 (1) (2017) 1.
[3] Reda A. Ammar, A.-N.M.A. Alaghaz, M.E. Zayed, L.A. Al-Bedair, J. Mol. Struct. 1141 (2017) 368.
[4] S. Shen, H. Chen, T. Zhu, X. Ma, J. Xu, W. Zhu, R. Chen, J. Xıe, T. Ma, L. Jia, Y. Wang, C. Peng, Oncol. Lett. 13 (2017) 3169.
[5] A. Zülfikaroğlu, Ç. Yüksektepe, H. Batı, N. Çalışkan, Russ. J. Coord. Chem. 36 (2) (2010) 124.
[6] A. Zülfikaroğlu, H. Batı, N. Dege, J. Mol. Struct. 1162 (2018) 125.
[7] S.A. Khan, S.A.A. Nami, S.A. Bhat, A. Kareem, N. Nishat, Microb. Pathog. 110 (2017) 414.
[8] Y. Gou, J. Li, B. Fan, B. Xu, M. Zhou, F. Yang, Eur. J. Med. Chem. 134 (2017) 207.
[9] D. Kumar, S. Chadda, J. Sharma, P. Surain, Bioinorgan. Chem. Appl. (2013) 1. Article ID 981764.
[10] J. Deng, W. Chen, H. Deng, J. Fluorese 26 (2016) 1987.
[11] S. Mahajan, B. Singh, H.N. Sheıkh, B.L. Kalsotra, Chem. Sci. Trans. 1 (1) (2012) 23.
[12] Wang Jing-lin, Zhao Ya-qin, Yang Bin-sheng, Inorg. Chim. Acta. 409 (2014) 484.
[13] K.S. Abou-Melha, Spectrochim. Acta, Part A 70 (2008) 162.
[14] M.S.A. Galil, A.N. Al-Hakimi, R.Y. Alshwafy, R.A.A. Okab, A. Mutir, Chemother. J. 1–3 (2015) 95.
[15] N. Chitrapriya, V. Mahalingam, M. Zeller, H. Lee, K. Natarajan, J. Mol. Struct. 984 (2010) 30.
[16] S.P. Dash, S. Pasayat, H.R. Dash, S. Das, R.J. Butcher, R. Dinda, Polyhedron 33 (1) (2012) 524.
[17] D. Hedge, G.N. Naik, R.S. Vadavi, V.S. Kumar, D.A. Barretto, K.B. Gudasi, Inorg. Chem. Acta 461 (2017) 301.
[18] A.S. El-Tabl, M.M.A. El-Waheed, M.A. Wahba, N.A.E.A.A. El-Fadl, Bioinorgan. Chem. Appl. 126023 (2015) 1.
[19] M. Rashidian, M.M. Mahmoodi, R. Sahah, J. Dozier, C.R. Wagner, M.D. Distefano, Bioconjugate Chem. 24 (2013) 333.
[20] N.M.H. Salem, L.E. Sayed, W. Haase, M.F. Iskander, Spectrochim. Acta, Part A 134 (2015) 257.
[21] R. Gup, E. Girizoğlu, Spectrochim. Acta, Part A 65 (2006) 719.
[22] R. Chaudhary, S. Shelly, Int. J. Pharm. Stud. Res. 2 (2011) 39.
[23] N.M.H. Salem, L.E. Sayed, W. Haase, M.F. Iskander, J. Coord. Chem. 58 (15) (2005) 1327.
[24] N.S. Al-Radadi, M.M. Akl, M.A. Elbeshlawi, M.M. Mostafa, Open J. Inorg. Chem. 6 (2016) 1.
[25] S. Naskar, S. Naskar, S. Mondal, P.K. Majhi, M.G.B. Drew, S.K. Chattopadhyay, Inorg. Chim. Acta. 371 (2011) 100.
[26] S. Gao, Z.P. Deng, L.H. Huo, H. Zhao, Acta Crystallogr. E61 (2005) o124.
[27] N.M.E. Metwally, A.A. El-Asmy, A.A. Abou-Hussen, Int. J. Pure Appl. Chem. 1 (1) (2006) 75.
[28] P. Kurnaz, C.Y. Ataol, H. Bati, O. Buyukgungor, Mol. Cryst. Liq. Cryst. 634 (2016) 61.
[29] H. Batı, M. Tas, C. Davran, Russ. J. Inorg. Chem. (Engl. Transl.) 51 (5) (2006) 728.
[30] F. Guntepe, M. Çınarlı, C. Kazak, H. Batı, Mol. Cryst. Liq. Cryst. 616 (1) (2015) 213.
[31] S. Naskar, D. Mishra, R.J. Butcher, S.K. Chattopadhyay, Polyhedron 26 (2007) 3703.
[32] E.A. Saad, M.M. Hassahien, F.W. El-Iban, Biochem. Bioph. Res. Co. 484 (2017) 579.
[33] S. Karadeniz, C.Y. Ataol, O. Sahin, O. Idil, H. Batı, J. Mol. Struct. 1161 (2018) 477.
[34] M.A. Mohammed, M.A. Moudar, J.M. Salim, Raf. J. Sci. (23) (2012) 51.
[35] G.M. Sheldrick, Acta Crystallogr. A71 (2015) 3.
[36] L.J. Farrugia, J. Appl. Crystallogr. 45 (2012) 849.
[37] G.M. Sheldrick, Acta Crystallogr. C71 (2015) 3.
[38] N. Sarı, N. Piskin, H. Ogutucu, N. Kurnaz, Med. Chem. Res. 22 (2013) 580.
[39] P. Prieto, M. Pineda, M. Aguilar, Anal. Biochem. 269 (2) (1999) 337.
[40] M. Oyaizu, Jpn. J. Nutr. Diet. 44 (6) (1986) 307.
[41] P.D. Duh, J. Am. Oil Chem. Soc. 75 (4) (1998) 455.
[42] M. Nishikimi, N.A. Rao, K. Yagi, Biochem. Bioph. Res. Co. 46 (2) (1972) 849.
[43] R. Re, N. Pellegrini, A. Proteggente, A. Pannala, M. Yang, C. Rice-Evans, Free Radical Biol. Med. 26 (9) (1999) 1231.
[44] J. Bernstein, R.E. Davis, L. Shimoni, N.-L. Chang, Angew Chem. Int. Ed. Engl. 34 (1995) 1555.
[45] A. Zülfikaroğlu, Ç. Yüksektepe, H. Batı, N. Çalışkan, O. Büyükgüngör, J. Struct. Chem. 50 (6) (2009) 1166.
[46] S. Mondal, C. Das, B. Ghosh, B. Pakhira, A.J. Blake, M.G.B. Drew, S.K. Chattopadhyay, Polyhedron 80 (2014) 272.
[47] N.M.H. Salem, L.E. Sayed, S. Foro, W. Haase, M.F. Iskander, Polyhedron 26 (2007) 4161.
[48] E. Canpolat, BEU J. Sci. 3 (1) (2014) 74.
[49] M. Sutradhar, E.C.B.A. Alegria, M.F.C. Guedes de Silva, L.M.D.R.S. Martins, A.J.L. Pombeiro, Molecules 21 (2016) 425.
[50] V.P. Singh, Spectrochim. Acta, Part A 71 (2008) 17.
[51] M.M.H. Khalil, E.H. İsmail, G.G. Mohammed, E.M. Zayed, A. Badr, Open J. Inorg. Chem. 2 (2012) 13.
[52] M. El-Behery, H. El-Twigry, Spectrochim. Acta, Part A 66 (2007) 28.
[53] M. Čačić, M. Molnar, B. Šarkanj, E. Has-Schön, V. Rajković, Molecules 15 (10) (2010) 6795.
[54] T. Özen, M. Tas, J. l of Enzy, Inh. Med. Chem. 24 (5) (2009) 1141.
[55] G.O. Puntel, P. Gubert, G.L. Peres, L. Bresolin, J.B.T. Rocha, M.E. Pereira, F.A. Soares, Arch. Toxicol. 82 (10) (2008) 755.
[56] A.T. Girgih, R. He, F.M. Hasan, C.C. Udenigwe, T.A. Gill, R.E. Aluko, Food Chem. 173 (2015) 652.
[57] H. Yu, X. Liu, R. Xing, S. Liu, C. Li, P. Li, Bioorg. Med. Chem. Lett 15 (10) (2005) 2659.
[58] A. Sadiq, F. Mahmood, F. Ullah, M. Ayaz, S. Ahmad, F.U. Haq, M.S. Jan, Chem. Cent. J. 9 (1) (2015) 31.